

# **Assimilation of GPS RO and its Impact on Numerical**

## **Weather Predictions in Hawaii**

Chunhua Zhou and Yi-Leng Chen

Department of Meteorology, University of Hawaii at Manoa, Honolulu, Hawaii

### **Abstract**

Assimilation of GPS (Global Positioning System) RO (Radio Occultation) refractivity based on WRF-3DVAR is applied to numerical weather predictions (NWP) in Hawaii, where limited conventional observations and poor representation of local circulations in global analysis restrains the quality of numerical weather predictions. With GPS RO refractivity assimilated, a cold front is better defined and the vertical profiles of temperature and moisture are largely improved compared to model runs without GPS RO assimilation. Another study of the trade wind inversion reveals that the trade wind inversion is better predicted with GPS RO assimilated.

### **1. Introduction**

The six Formosa Satellite Mission 3/Constellation Observing System for Meteorology, Ionosphere, and Climate (FORMOSAT-3/COSMIC) microsattellites carry global positioning system (GPS) radio occultation (RO) receivers to measure the phase and amplitude of GPS signals (Anthes et al. 2000, 2008). These data can be

used to obtain vertical profiles of bending angle, atmospheric refractivity (Kuo et al 2004) and atmospheric soundings (Kirsinski et al. 1997). Unlike satellite data such as AIRS (Atmospheric Infrared Sounder) measurements, which might not be good under cloudy skies, GPS RO data can provide high-vertical-resolution all-weather refractivity profiles and hence high-vertical-resolution temperature and humidity profiles (Yunck et al. 2000, Ho et al 2007). Previous studies have shown positive impacts of GPS RO on numerical weather predictions. Huang et al (2005) utilized MM5 (the fifth-generation Pennsylvania State University-National Center for Atmospheric Research Mesoscale Model) and 3DVAR (three dimensional variational data assimilation) to study the impacts of GPS RO refractivity on simulating typhoons Nari (2001) and Nakri (2002) and found improved 24-hour accumulated rainfall prediction for both typhoons. Wee et al (2008) investigated the impacts of GPS RO on short-range forecasts over the Antarctic using MM5-4DVAR (four dimensional variational data assimilation). Their results show positive or near neutral impact for assimilation over a single 12-h period. On the other hand, considerable positive impacts are found throughout the model atmosphere when extending the assimilation to 48 hours. Beginning in 2007, scientists at NCEP (National Centers for Environmental Prediction) implemented GPS RO into their Global Data Assimilation System (GDAS) (Cucurull et al 2007, 2008; Cucurull and Derber 2008) and made these data available to the public.

Located in the mid-Pacific Ocean, with limited conventional in situ observations, the Hawaiian Island chain is an excellent place to test the impact of

remotely sensed satellite data on high-resolution weather modeling. Many previous studies have simulated island circulations under different trade-wind regimes and their response to various island terrains over the Hawaiian Islands with different initial conditions. Chen and Feng (2001) performed model simulations initialized by a single sounding. For real case studies, Zhang et al. (2005a, b) and Yang et al. (2005) initialized their models with the NCEP/NCAR (National Center for Atmospheric Research) global analysis whereas several other studies (Yang et al, 2008; Yang and Chen 2008; Nguyen et al 2010; Carlis et al 2010) initialized their models with the NCEP GFS (Global Forecast System) model output.

Chen and Feng (1995) examined rainfall patterns over the Island of Hawaii (Big Island) under high and low trade-wind inversions during the Hawaiian Rainband Project (HaRP). Their results suggested that for the low- (high-) inversion days, the median daily rainfall on the windward side of the Big Island is about one-half (more than twice) of the HaRP median daily rainfall. Using MM5, Chen and Feng (2001) simulated island airflow and weather under summer trade-wind conditions. They showed that the trade-wind inversion height represents the depth of the moist layer that affects cloud development and convective feedback to the island airflow. For mountains with tops well above the trade-wind inversion, the inversion also serves as a lid forcing the low-level airflow to move around the terrain (Leopold 1949; Chen and Feng 2001). An accurate depiction of the trade-wind inversion is therefore crucial for properly simulating island airflow and cloud distributions under summer trade-wind conditions over the Hawaiian Islands.

In this study, GPS RO data from the NCEP GDAS are assimilated in the regional domains over the Hawaiian Islands using WRF (Weather Research and Forecasting Model)-3DVAR to improve the initial conditions provided by the NCEP Final Analysis (FNL). The impacts of GPS RO on regional numerical simulations over the Hawaiian Islands will be investigated. Two cases, a winter cold front and a summer trade-wind case, are selected. For the winter cold front case, we would like to assess the impacts of assimilating GPS RO on the movement and evolution of the simulated cold front. For the trade-wind case, we would like to assess the impacts of assimilating GPS RO on simulating the vertical structure trade-wind inversion.

## **2. Data and experimental design**

WRF-3DVAR is used to assimilate the GPS RO data for numerical weather predictions in Hawaii. Model initial conditions and lateral boundary conditions come from NCEP FNL (Final) Operational Model Global Tropospheric Analyses continuously at every six hours, with a  $1^\circ \times 1^\circ$  horizontal resolution and 26 vertical levels. A daily high-resolution global sea surface temperature (RTG\_SST) analysis developed at the NCEP/Marine Modeling and Analysis Branch (NCEP/MMAB) is also used to provide the lower boundary conditions. GPS RO data come from NCEP/GDAS in BUFR format, downloaded from the NOAA nomads (National Operational Model Archive and Distribution System) server (<http://nomads.ncdc.noaa.gov/data/gdas/>). For forecast verification, total precipitable water (TPW) from AIRS measurements, FNL and the skew-T plots at Lihue (21.98°N, 159.35°W) on the Island of Kauai and Hilo (19.71°N, 155.06°W) on the Big Island are

compared with the model results.

The model includes three domains with 18-, 6- and 2-km horizontal spacings, respectively (Fig.1), and 38 vertical levels. The Hawaiian Islands are characterized by large variations in terrain heights, vegetation types, and soil types (Zhang et al 2005, Yang et al 2005, Nguyen et al 2010). In this study, the land use, soil type and vegetation fraction data are from Zhang et al. (2005a) and the Noah land surface model is used.

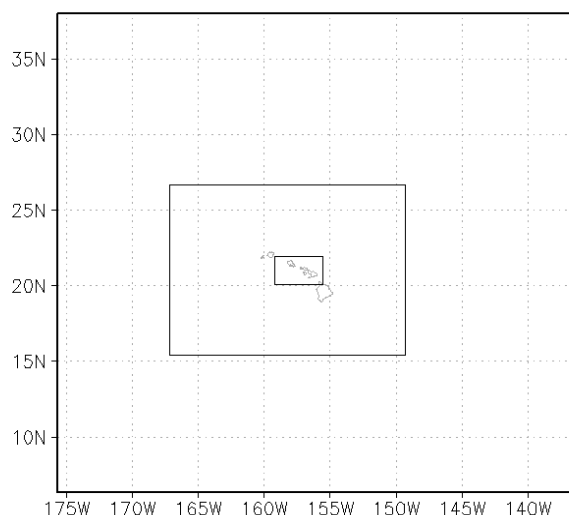


Fig.1 Locations of the three domains, with 18km, 6km and 2km horizontal spacings respectively.

Two sets of experiments are designed, with and without GPS RO assimilation. For the one with GPS RO assimilation, starting at 12UTC, the model is first integrated for 12 hours. At 00UTC, GPS RO refractivity data is applied to the 12-hour forecast field through WRF-3DVAR with a +/- 3-hour time window. After assimilation of GPS RO, the hereby updated fields are integrated for another 2 days and the forecast fields are compared with those without the assimilation of GPS RO

data.

During the period of January 29 to January 31, 2010, a cold front approached the Hawaiian Islands and brought heavy rainfall to most islands. The model is initialized at 12UTC January 28, 2010. For the no-GPS RO run, the model is integrated to 00UTC January 31, 2010. For the run with GPS RO assimilation, WRF-3DVAR is performed at the 12-hour forecast field (valid at 00 UTC January 29, 2010) and the updated fields are integrated to 00UTC January 31, 2010. The period of September 6 to September 8, 2009 is selected to study the impact of GPS RO data on the simulation of trade-wind inversion. The model is initialized at 12UTC September 5, 2009 and integrated to 00UTC September 8, 2009 for the no-GPS RO run. For the GPS RO run, the assimilation takes place at 00UTC September 6, 2009.

### **3. Impact of assimilating GPS RO in a cold front event**

As pointed out by previous studies (Kuo et al 2004, Huang et al 2005, Ho et al 2007), the high-vertical-resolution profiles of GPS RO refractivity have positive impacts on numerical weather predictions. With a cold front, we expect the detailed temperature and humidity profiles from GPS RO data would produce a more defined cold front and more accurate rainfall distribution along with it.

As the assimilation of GPS RO is performed at 00UTC January 29, 2010, we'd like to examine the forecast field 24 hours or longer after the assimilation, which includes the 36-hour (valid at 00UTC January 30, 2010), 48-hour (valid at 12UTC January 30, 2010) and 60-hour (valid at 00UTC January 31, 2010) forecasts. Fig.2



of the frontal zone, with maximum TPW reaching the island of Maui. It is clear that with GPS RO assimilated, the movement of the axis of maximum TPW associated with cold front is better simulated.

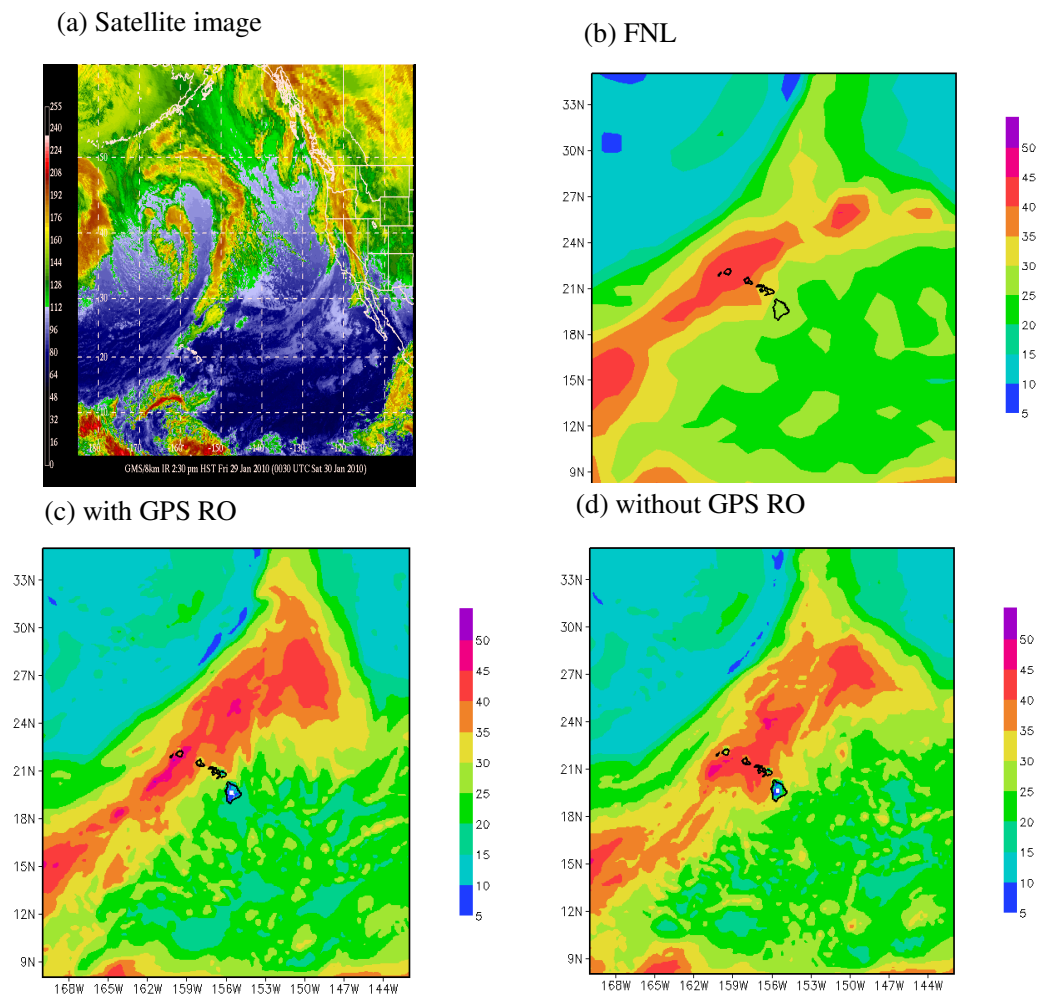


Fig.3 (a) Satellite image at 00:30UTC January 30, 2010; (b) Total Precipitable Water ( $kg/m^2$ ) at 00UTC January 30, 2010 from NCEP FNL; (c) Total Precipitable Water at 00UTC January 30, 2010 from the GPS RO run; (d) Total Precipitable Water at 00UTC January 30, 2010 from the no-GPS RO run.

Fig.4 is similar to Fig.3, except the modeled fields are 48-hour forecasts valid at 12UTC January 30, 2010. From the satellite image, the cloud system now moves eastward and covers from east of Kauai to Maui. The TPW field from NCEP FNL

shows a similar distribution as the satellite image, with large TPW covering the same region. Comparison of the modeled TPW with the cloud distribution and the observed TPW shows that with GPS RO assimilated, the spatial pattern of the TPW is closer to the observed, mainly covering the area from Oahu to Maui, while the TPW from the no-GPS RO run is further east, with large values reaching the Big Island.

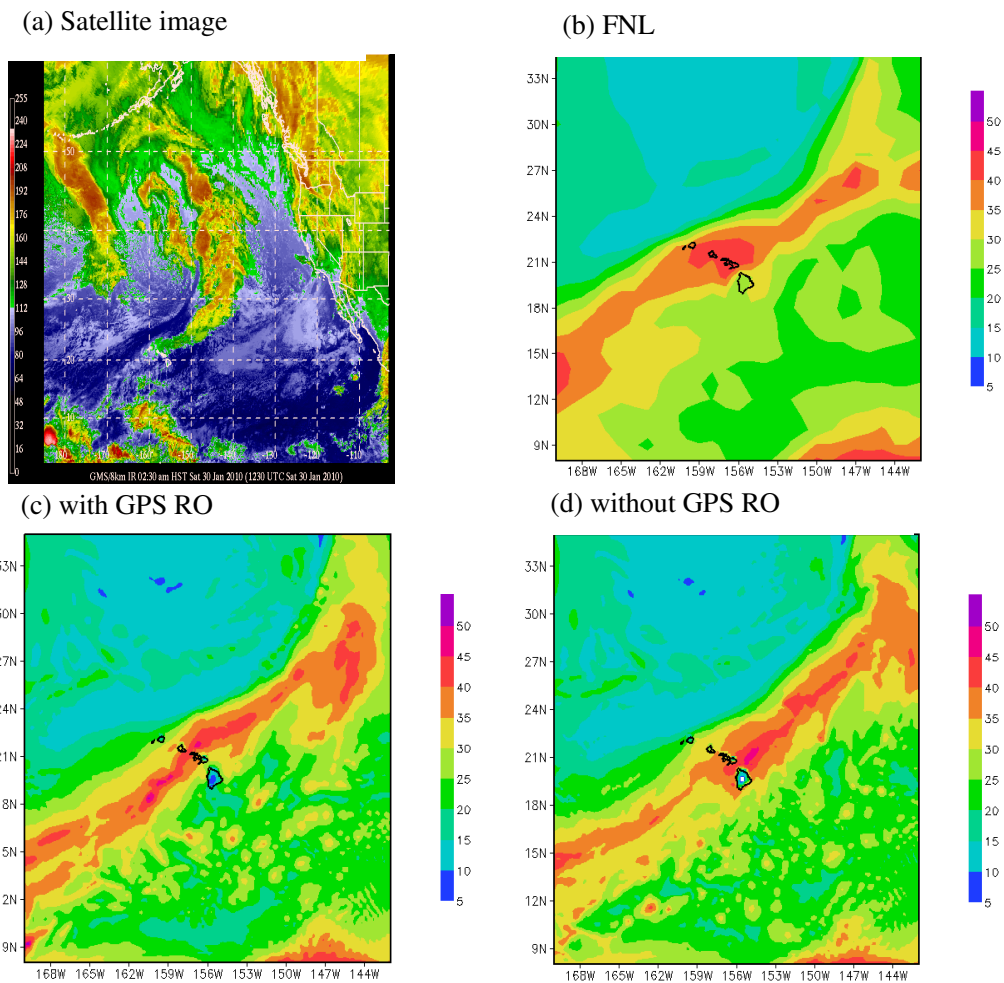


Fig. 4 Similar to Fig.3, valid at 12UTC January 30, 2010.

Fig.5 gives the TPW fields from AIRS measurements (a), NCEP FNL (b) and the 60-hour forecast (c) and (d) at 00UTC January 31, 2010. Consistent with what Fig.3 and Fig.4 have suggested, the modeled TPW with GPS RO assimilation gives a

more realistic spatial distribution of the TPW field while the no-GPS RO run tends to produce large values of TPW further east. The above time series of TPW fields at 36-hour (Fig.3), 48-hour (Fig.4) and 60-hour (Fig.5) all point out that assimilation of GPS RO improves the predictions of the cold front position as well as producing a better simulation of spatial distribution of TPW associated with the propagation of the cold front.

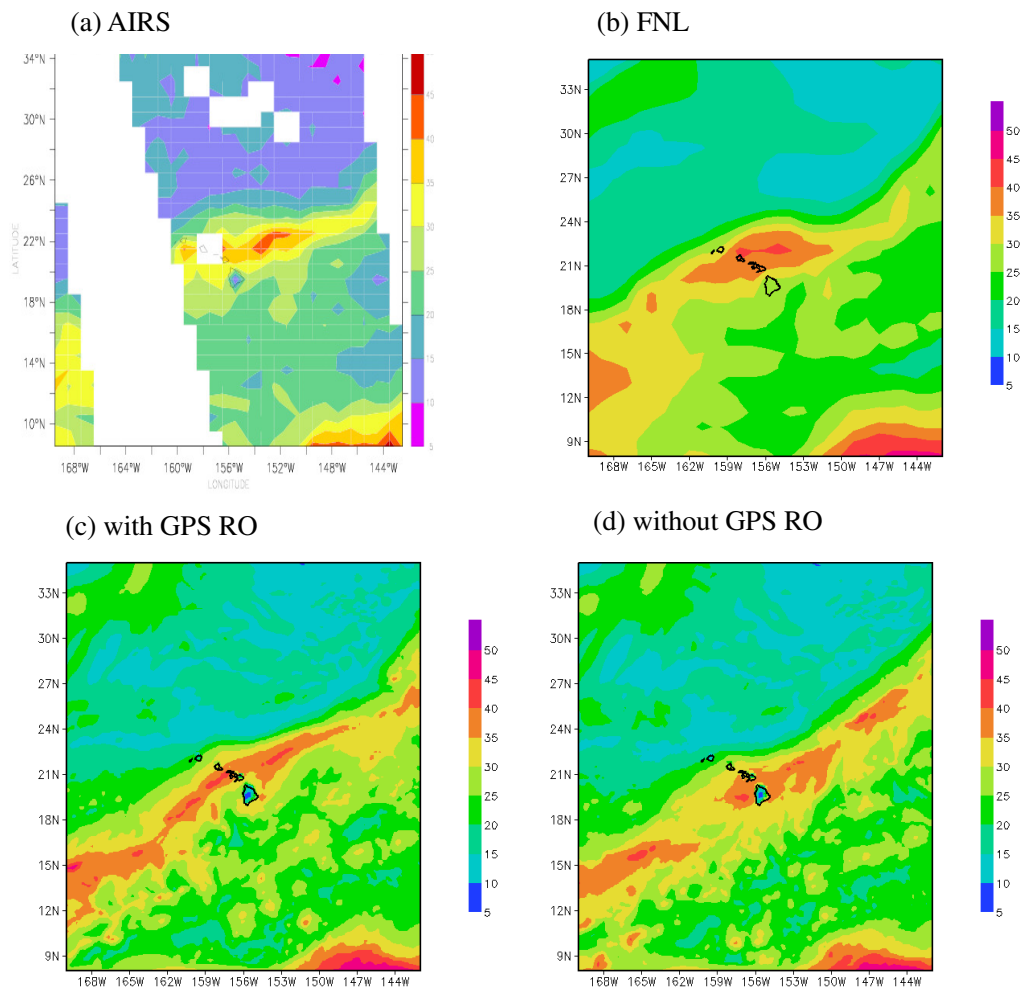


Figure 5 (a) Total column water vapor at 23:30 UTC 30, 2010, from AIRS measurements; (b) TPW at 00 UTC 31, 2010 from NCEP FNL; (c) TPW at 00 UTC 31, 2010 from the GPS RO run; (d) TPW at 00 UTC 31, 2010 from the no-GPS RO run.

How about the vertical profiles in the GPS RO and no-GPS RO runs compared to the observations? Fig.6 gives the skew-T plots for Lihue at 00UTC January 30 and 31, 2010, downloaded from the University of Wyoming. The air at Lihue was very moist for the entire column from surface to around 500hPa on January 30, 2010, suggesting deep convection may have been present with cloud tops reaching up to 500hPa. This is consistent with the surface analysis and the TPW field from NCEP FNL, in which Kauai is right ahead of the cold front with large values of TPW. By 00UTC Jan. 31, 2010, the front has moved to the island of Oahu and the convection is weakening over the island of Kauai, as can be seen from the skew-T plot that shows the air is less moist as compared to the previous day, especially above 700hPa.

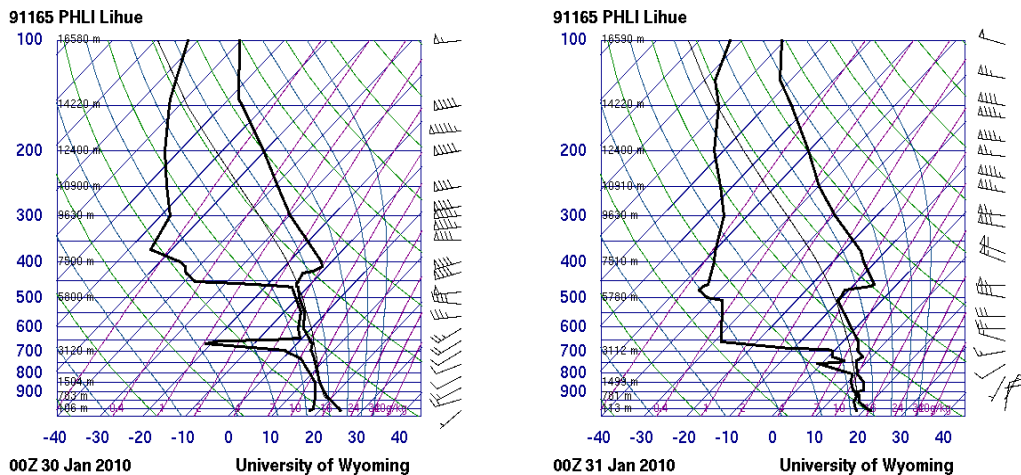


Figure 6 Skew-T plots at Lihue, valid at 00UTC January 30 (left) and 31 (right), 2010. The black thick line on the left (right) of each panel represents the profile of temperature (dew point temperature). These figures were downloaded from the University of Wyoming (<http://weather.uwyo.edu/upperair/sounding.html>).

Next we take a look at our model results and see which experiment simulates a

more realistic atmospheric vertical profile. Skew-T plots are produced for the Lihue station for both experiments. Fig. 7 gives the skew-T plot from the experiment without GPS RO assimilation. We can see the depth of the moist air at 00UTC January 30, 2010 is largely underestimated, only up to around 700hPa, compared to the observed moist layer up to 500hPa. By 00UTC January 31, the air is very dry for Lihue, which is inconsistent with the observed profile.

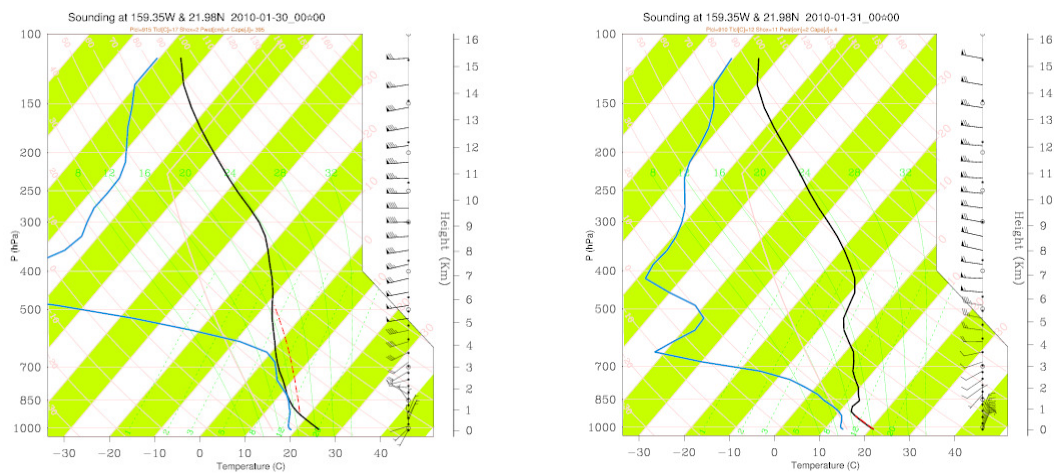


Figure 7 Skew-T plots at Lihue valid at 00UTC January 30 (left) and 31 (right), 2010, based on the experiment without GPS RO assimilation. The black (blue) thick line represents the temperature (dew point temperature) profile.

Fig. 8 gives the skew-T plots at Lihue based on the experiment with GPS RO assimilation. Compared to the experiment without GPS RO assimilation, the depth of the moist air is deeper and closer to that which is observed. The convection reaches above 600hPa at 00UTC January 30, 2010. Although the simulated depth of the moist layer is still underestimated compared to the observations, we see significant improvements when assimilating GPS RO. By 00UTC January 31, 2010, the lower

tropospheric atmosphere is slightly more moist than that without GPS RO, even though both experiments underestimate the moisture compared with the observations.

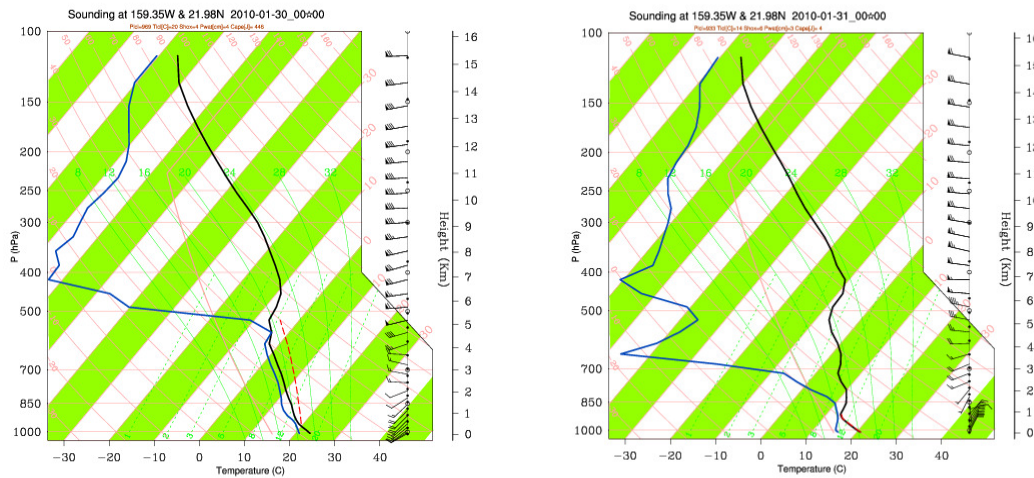


Figure 8 Skew-T plots at Lihue, valid at 00UTC January 30 (left) and 31 (right), 2010, based on the experiment with GPS RO assimilation. The black (blue) thick line represents the temperature (dew point temperature) profile.

The above analysis shows that the vertical thermodynamic profiles are better simulated with GPS RO assimilation, in addition to the improved simulations of the spatial distributions of TPW associated with the propagation of the cold front. These results are consistent with previous studies in suggesting that the assimilation of GPS RO does improve numerical weather simulations for Hawaii.

#### 4. Assimilating GPS RO in a trade wind case

In this section, we conduct two experiments with or without GPS RO assimilation for the period of September 6 to September 8, 2009. We use skew-T plots at the two sounding stations to verify the model results. Fig.9 gives the observed

temperature and dew point temperature profile at 12UTC September 7, 2009 at Lihue in the upper panel and the modeled profiles from the experiments with (left) and without (right) GPS RO assimilation. The observed trade-wind inversion, denoted by inversed temperature gradient and sharp decrease of the dew point temperature (humidity), is at about 700 hPa. The skew-T plot with GPS RO assimilation gives the trade wind inversion at about 700 hPa and below while the skew-T plot without GPS RO assimilation gives no trade-wind inversion at all.

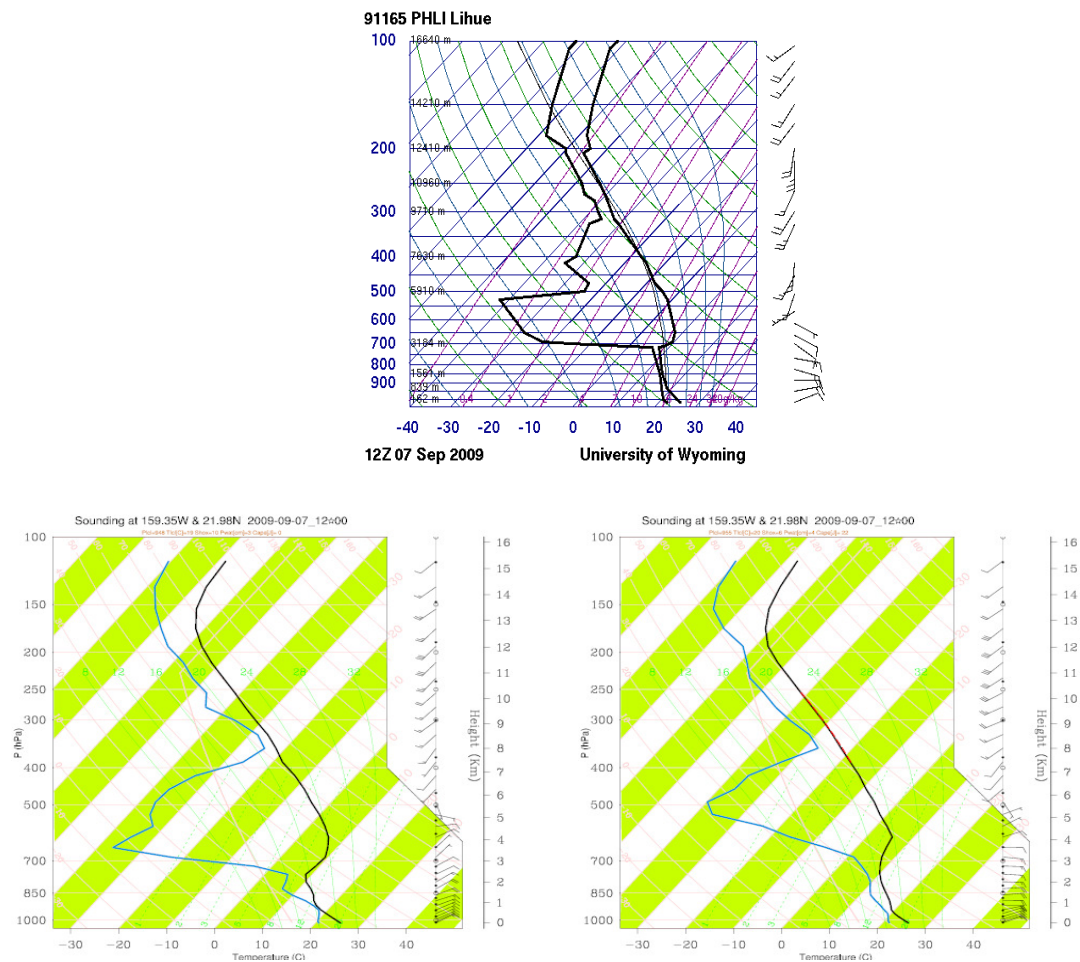


Fig. 9 Upper panel: observed skew-T plot at Lihue downloaded from University of Wyoming; lower panels: skew-T plots at Lihue from the experiments with (left) and without (right) GPS RO assimilation. All the plots are valid at 12UTC September 07, 2009.

Fig. 10 gives the skew-T plots at Hilo at 12 UTC September 7, 2009. Observations (upper panel) show a trade-wind inversion between 800 hPa and 700 hPa. The air is very moist below the trade-wind inversion. The experiment with GPS RO assimilation simulates a trade-wind inversion between 750 hPa and 650 hPa, below which the air is moist. On the other hand, the experiment without GPS RO assimilation gives no trade-wind inversion and the lower troposphere is dryer than the observed. Both Fig.9 and Fig.10 give better simulations of the trade-wind inversions with GPS RO assimilation.

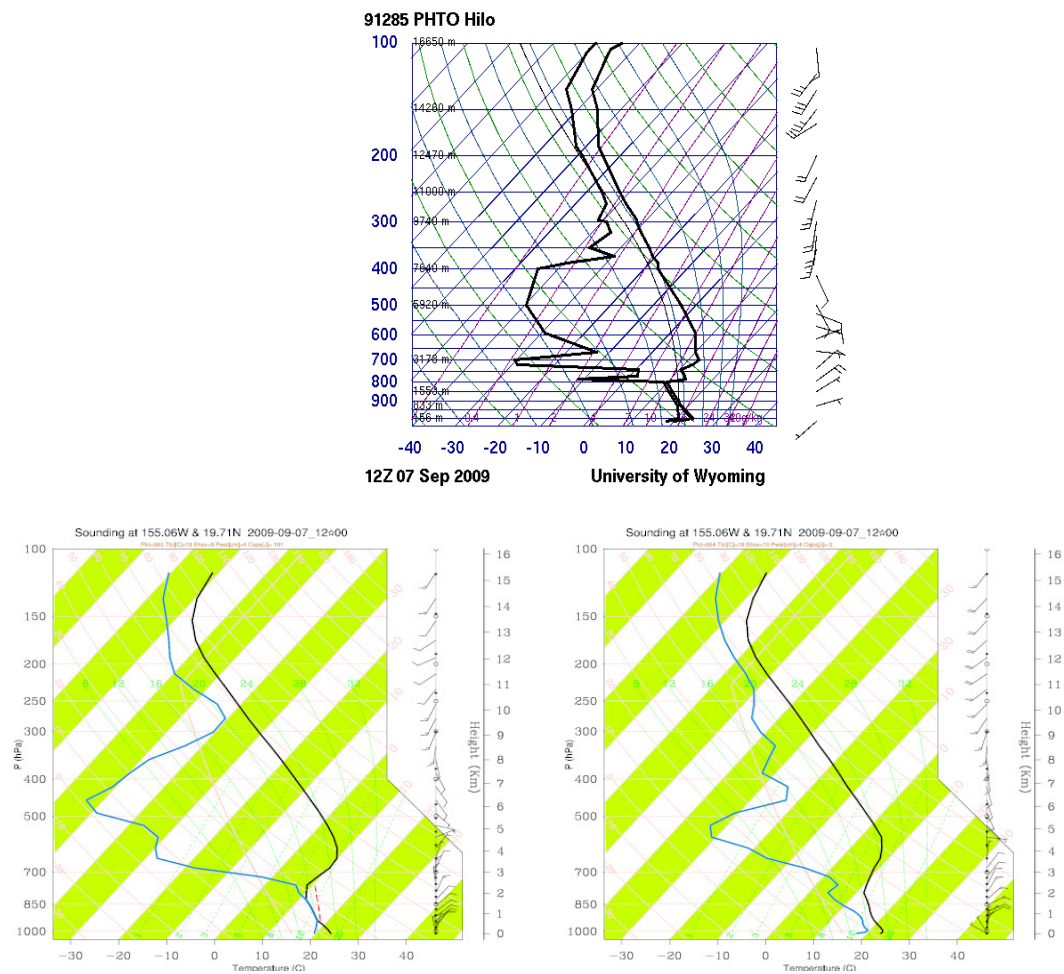


Fig. 10 Same as Fig.9, except for Hilo.

## 5. Conclusions

GPS RO refractivity data are assimilated using WRF-3DVAR and its impacts on numerical weather simulations in Hawaii are investigated. Two typical scenarios are chosen, a winter cold front case and a summer trade-wind case, to study the effects of GPS RO assimilation under different weather conditions.

With the more detailed information of temperature and humidity profiles from the GPS RO data, the model produces a better defined cold front, with better simulated deep convection and spatial distribution of the TPW, as compared to the model without GPS RO assimilation. The study of a trade-wind case lends support to the improvements on numerical weather predictions through assimilating GPS RO. In this case, trade-wind inversions are better simulated with GPS RO assimilation than without GPS RO assimilation. Both cases are consistent with previous studies, showing positive impacts of GPS RO on the numerical weather simulations over the Hawaiian Islands.

**Acknowledgement:** We'd like to thank DTC for hosting the visit to NCAR and the staff in DTC for their help. Special thanks to Dr. Xiang-Yu Huang and Dr. Louisa Nance for their help on the WRF-3DVAR.

## References

Anthes, R.A., C. Rocken, and Y.-H. Kuo, 2000: Application of COSMIC to meteorology and climate, *Terr. Atmos. Oceanic Sci.*, 11, 115-156.

-----, R. A., D. Ector, D. C. Hunt, Y.-H. Kuo, C. Rocken, W. S. Schreiner, S. V. Sokolovskiy, S. Syndergaard, T-K. Wee, Z. Zeng, P. A. Bernhardt, K. F. Dymond, Y. Chen, H. Liu, K. Manning, W. J. Randel, K. E. Trenberth, L. Cucurull, S. B. Healy, S-P. Ho, C. McCormick, T. K. Meehan, D. C. Thompson, N. L. Yen, 2008: The COSMIC/FORMOSAT-3 Mission: Early Results, *Bull. Amer. Meteor. Soc.*, 89 (3), 313-333.

Carlis, D., L., Y.-L. Chen, and V. Morris, 2010: Numerical simulations of island-scale airflow and the Maui vortex during summer trade-wind conditions. *Mon. Wea. Rev.*, In Press.

Chen, Y.-L., and J. Feng, 1995: The influences of inversion height on the precipitation and airflow over the island of Hawaii. *Mon. Wea. Rev.*, **123**, 1660-1676.

Chen, Y.-L., and J. Feng, 2001: Numerical simulations of airflow and cloud distributions over the windward side of the island of Hawaii. Part I: The effects of trade-wind inversion. *Mon. Wea. Rev.*, **129**, 1117-1134.

Cucurull, L., J. C. Derber and R. Treadon, R. J. Purser, 2007: Assimilation of Global Positioning System Radio Occultation Observations into NCEP's Global Data Assimilation System, *Mon. Wea. Rev.*, 135: 3174-3193.

-----, -----, and -----, -----, 2008: Preliminary Impact Studies Using Global Positioning System Radio Occultation Profiles at NCEP. *Mon. Wea. Rev.*, **136**,

1865-1877.

-----, -----, 2008: Operational Implementation of COSMIC Observations into NCEP's Global Data Assimilation System. *Wea. Forecasting*, **23** (4), 702-711.

Ho, S.-P., Y.-H. Kuo, S. Sokolovskiy, 2007: Improvement of the Temperature and Moisture Retrievals in the Lower Troposphere Using AIRS and GPS Radio Occultation Measurements, *J. Atmos. Oceanic Technol.*, **24**, 1726-1739.

Huang, C.-Y., Y.-H. Kuo, S.-H. Chen, F. Vandenberghe, 2005: Improvements in Typhoon Forecasts with Assimilated GPS Occultation Refractivity, *Wea. Forecasting*, **20**, 931-953.

Kuo, Y.-H., T. K. Wee, S. Sokolovskiy, C. Rocken, W. Schreiner, D. Hunt, and R. A. Anthes, 2004: Inversion and error estimation of GPS radio occultation data. *J. Meteor. Soc. Japan*, **82B**:507–531.

Kuo, Y.-H., W. S. Schreiner, J. Wang, D. L. Rossiter, and Y. Zhang, 2005: Comparison of GPS radio occultation soundings with radiosondes. *Geophys. Res. Lett.*, **32**.L05817, doi:10.1029/2004GL021443.

Kursinski, E. R., G. A. Hajj, J. T. Schofield, R. P. Linfield, and K. R. Hardy, 1997: Observing earth's atmosphere with radio occultation measurements using the global positioning system. *J. Geophys. Res.*, **102**:D19. 23429–23465.

Leopold, L. B., 1949: The Interaction of Trade Wind and Sea Breeze, Hawaii. *J. Meteor.*, **6**, 312 – 320.

Nguyen, H. V., Y.-L. Chen, and F. Fujioka, 2010: Numerical Simulations of island effects on airflow and weather during the summer over the Island of Oahu. *Mon. Wea.*

Rev., In Press.

Wee, T.-K., Y.-H. Kuo, D. H. Bromwich, A. J. Monaghan, 2008: Assimilation of GPS Radio Occultation Refractivity Data from CHAMP and SAC-C Missions over High Southern Latitudes with MM5 4DVAR, *Mon. Wea. Rev.*, **136**, 2923-2944.

Yang, Y., Y.-L. Chen, and F. M. Fujioka, 2005: Numerical simulations of the island-induced circulation over the island of Hawaii during HaRP. *Mon. Wea. Rev.*, **133**, 3693-3713.

-----, and -----, 2008: Effects of terrain heights and sizes on island-scale circulations and rainfall for the island of Hawaii during HaRP. *Mon. Wea. Rev.*, **136**, 120-146.

-----, -----, and F. M. Fujioka, 2008: Effects of trade-wind strength and direction on the leeside circulations and rainfall of the island of Hawaii *Mon. Wea. Rev.*, **136**, 4799-4818.

Yunck, T., C-H. Liu, and R. Ware, 2000: A history of GPS sounding. *Terr. Atmos. Oceanic Sci.*, **11**, 1-20.

Zhang, Y., Y.-L. Chen, S.-Y. Hong, H.-M. H. Juang, and K. Kodama, 2005: Validation of the coupled NCEP Mesoscale Spectral Model and an advanced Land Surface Model over the Hawaiian Islands. Part I: Summer trade wind conditions and a heavy rainfall event. *Wea. Forecasting*, **20**, 847-872.

-----, -----, and K. Kodama, 2005: Validation of the coupled NCEP Mesoscale Spectral Model and an advanced Land Surface Model over the Hawaiian Islands. Part II: A high wind event. *Wea. Forecasting*, **20**, 873-895.